Materials Today Bio 16 (2022) 100339

Contents lists available at ScienceDirect

Materials Today Bio

journal homepage: www.journals.elsevier.com/materials-today-bio

Electrostatically optimized adapalene-loaded emulsion for the treatment of acne vulgaris

Yun Bae Ji [a,1], Hye Yun Lee [a,1], Soyeon Lee [a], Young Hun Kim [a], Kun Na [b], Jae Ho Kim [a], Sangdun Choi [a], Moon Suk Kim [a,c,*]

[a] Department of Molecular Science and Technology, Ajou University, Suwon, 443-749, South Korea
[b] Department of Biotechnology, The Catholic University of Korea, Bucheon, 420–743, South Korea
[c] Research Institute, Medipolymers, Suwon, 16522, South Korea

ARTICLE INFO

Keywords:
Electrostatic interaction
Adapalene
Electrostatic emulsifier
Emulsion
Acne vulgaris

ABSTRACT

Adapalene (AD) is an FDA-approved drug that shows good therapeutic efficacy for the treatment of acne vulgaris. However, due to its negative charge, AD cannot efficiently penetrate across the also negatively-charged skin membrane. This study is the first to assess the treatment of acne vulgaris using electrostatically optimized AD emulsions prepared using anionic AD with methoxy polyethylene glycol-*b*-poly(ε-caprolactone) (MC) as an anionic emulsifier coupled with a newly synthesized MC with different contents of an amine pendant-group (MC-$[NH_2]_x$) as a cationic emulsifier. The AD emulsion prepared using MC-$[NH_2]_x$ with high cationic charge potential was significantly stable in the short-term studies compared with anionic MC or no emulsifier. Furthermore, the AD emulsion prepared with the cationic MC-$[NH_2]_x$ emulsifier provided a two or three times stronger therapeutic effect against acne vulgaris than the AD emulsion prepared with the anionic MC emulsifier or no emulsifier in an animal study. Additionally, the AD emulsion with high cationic charge potential exerted a remarkable inhibition of macrophage expression, as confirmed by histological analysis. Therefore, the electrostatic interaction between the negatively-charged skin membrane and the AD emulsion prepared with the cationic MC-$[NH_2]_x$ emulsifier provides a promising therapeutic strategy for acne vulgaris.

1. Introduction

Acne vulgaris is among the most common dermatological diseases and can develop at all ages. The onset of acne vulgaris is caused by an increase in sebum production, which provides a substrate for the growth of bacteria such as *Propionibacterium acnes* in normal skin [1].

Topical therapy is typically the first line of treatment for mild and moderate the several skin diseases including acne vulgaris [2]. However, in severe cases, this therapy must be complemented with other conventional treatments. Topical retinoids including adapalene, tretinoin, and isotretinoin are among the most popular drugs that target the abnormal proliferation and differentiation of keratinocytes, in addition to possessing anti-inflammatory effects [3]. Among several topical retinoids, adapalene (AD) has become widely used for the topical treatment of acne vulgaris due to its minimal side effects, good efficacy, and favorable tolerability profile [4]. Due to these characteristics, AD has been reported to significantly improve inflammatory lesions as a safe treatment in clinical studies. Furthermore, several recent studies have described the preparation of AD-based topical treatments for acne vulgaris [5–7]. Additionally, most topical retinoids including AD possess negative groups in their molecular structure.

Over the last few decades, there has been significant progress in transdermal drug delivery as a means to facilitate the skin penetration of drugs [8–11]. Transdermal drug delivery has several advantages, including reduced side effects associated with gastrointestinal absorption and hepatic pass metabolism, as well as improved patient compliance.

Nevertheless, many drugs cannot easily diffuse through the skin because the stratum corneum of the skin possesses a high proportion of negative charges [12,13]. Therefore, the effectiveness of transdermal drug delivery is greatly influenced by the electrical charges associated with the molecular structure of the drug candidate, as this factor determines skin permeation.

Emulsions are among the most common and effective drug delivery systems for uniform deposition onto the skin, allowing for rapid drug

* Corresponding author. Department of Molecular Science and Technology, Ajou University, Suwon, 443-749, South Korea.
E-mail address: moonskim@ajou.ac.kr (M.S. Kim).
[1] Yun Bae Ji and Hye Yun Lee are equal first authors.

https://doi.org/10.1016/j.mtbio.2022.100339
Received 29 April 2022; Received in revised form 17 June 2022; Accepted 18 June 2022
Available online 24 June 2022

penetration across the skin, as well as prolonged skin-targeted effects [14–17]. Emulsions are colloidal dispersions of a liquid in another immiscible liquid stabilized using solubilizing oil molecules with a mixture of surfactants, co-surfactants, and co-solvents.

The formed emulsions can maintain a small and uniform droplet size with little probability of coalescence and flocculation as thermodynamically and kinetically stable systems. The spontaneous formation of emulsions with low interfacial energy and small size can be adjusted by the properties of several surfactants and/or emulsifiers (i.e., a broader classification of surfactant compounds or surface-active agents).

Previous studies have reported the use of emulsions for the treatment of acne vulgaris [18–20]. Particularly, recent studies have demonstrated that nano- and micro-emulsions constitute promising therapies against acne vulgaris [21–23]. Therefore, our study sought to prepare AD-loaded emulsions (AD emulsions) for the treatment of acne vulgaris.

Nonetheless, the negative potential charge of AD itself reduces its skin penetration efficacy, as well as the charge properties of the AD emulsions after preparation [24]. To address these limitations, the ionic properties of surfactants and/or emulsifiers may be used to modify the charge of the formed emulsion.

Recently, our group prepared an amphiphilic diblock copolymer of methoxy polyethylene glycol-*b*-poly(ε-caprolactone) (MC) with a slight anionic zeta potential charge [25], and this MC copolymer can act as an anionic emulsifier. More recently, we developed amphiphilic diblock copolymers with an amine pendant group (MC-NH_2) [26]. MC-NH_2 with different amounts of amine pendant groups (MC-[NH2]$_x$) as polyelectrolytes can form attractive or repulsive electrostatic interactions with oppositely or equally charged electrolytes, including drugs with charge potentials.

Based on the aforementioned observations, we hypothesized that MC with negative charge potential and MC-$[NH_2]_x$ with positive charge potential could act as electrostatic emulsifiers and thus electrostatically interact with AD, which has a negative charge potential. We then hypothesized that the electrostatically optimized AD and MC or MC-$[NH_2]_x$ can affect the stabilization of AD inside AD emulsions (Fig. 1).

To the best of our knowledge, no previous studies have reported the preparation of emulsions using MC-$[NH_2]_x$ copolymers as a cationic emulsifier. In the first half of this work, AD emulsions were prepared using MC or MC-$[NH_2]_x$ with different amounts of an amine pendant group, after which their charge was characterized. Additionally, *in vitro* cytotoxicity assays were also performed, followed by an animal study using AD emulsions with different charge potentials to assess their efficacy against acne vulgaris.

The objectives of the current study were: (1) to evaluate whether AD, an anionic drug, could form electrostatic interactions with an anionic MC emulsifier or cationic MC-$[NH_2]_x$ emulsifier, thus rendering AD emulsions; (2) to examine whether the formed AD emulsions were time- and temperature-stable; and (3) to determine whether the AD emulsions prepared with MC or MC-$[NH_2]_x$ are effective treatments against acne vulgaris.

2. Materials and methods

2.1. Materials

Methoxy polyethylene glycol (MPEG; number average molecular weight M_n = 750 g/mol), 1.0 M HCl in diethyl ether, 10 wt% palladium on carbon (Pd/C), 4-nitrophenyl chloroformate, triethylamine, 1,4-diaminobutane, adapalene, glycerin, caprylic/capric triglyceride oil (CCT oil), tetraglycol, and Tween 80 were purchased from Sigma-Aldrich (St. Louis, MO, USA). ε-Caprolactone (CL, TCI, Tokyo, Japan) was sequentially distilled from $CaCl_2$ and CaH_2 under nitrogen before use.

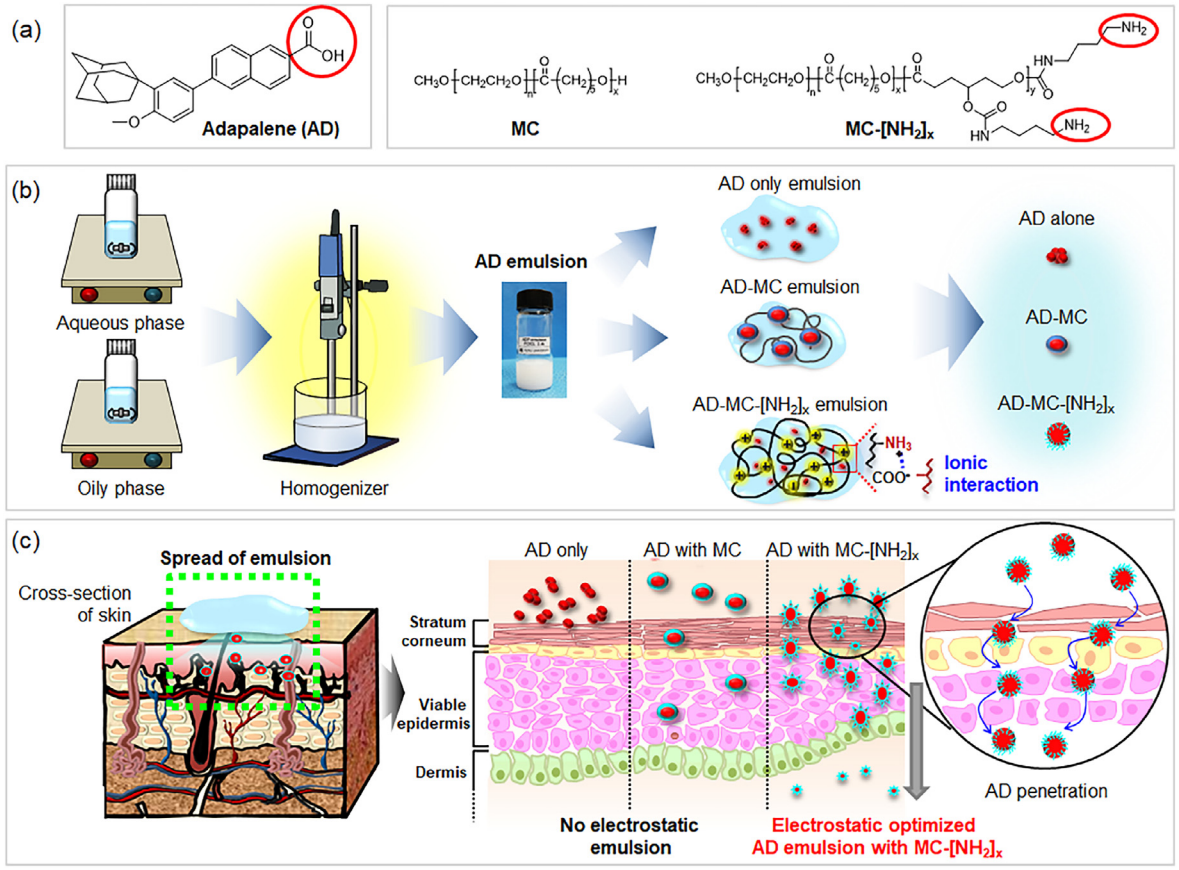

Fig. 1. Schematic representation of (a) adapalene (AD), the anionic MC copolymer and cationic MC-$[NH_2]_x$ copolymer; (b) preparation of AD emulsion (AD only emulsion, AD-MC emulsion using MC, and AD-MC-$[NH_2]_x$ emulsion using MC-$[NH_2]_x$); and (c) skin permeation of each AD emulsion.

Chloroform-D and acetone-D were purchased from Cambridge Isotope Laboratories, Inc. (MA, USA). Toluene, dichloromethane, *n*-hexane, ethyl ether, anhydrous tetrahydrofuran (THF), ethyl acetate (EA), celite, acetone, HCl (35.0%–37.0% in deionized water), magnesium sulfate ($MgSO_4$), and xylene were purchased from Samchun (Gyeonggi, Korea). Ethanol was purchased from Burdick & Jackson (MI, USA). Steareth-21, composed of polyethylene glycol ethers of stearic acid (PEG-100 stearate), was purchased from Clariant (Houston, TX). Divinyl dimethicone and silica silylate were obtained from Dow Corning (Seneffe, Belgium). Deionized water (DW) was prepared with an Ultra-Pure System (Romax, Hanam, Korea). Chloroform was purchased from J.T. Baker (Phillipsburg, NJ, USA).

2.2. Characterization

Using a Varian Mercury Plus 400 spectrophotometer (Varian), the ^1H NMR spectra of $(CD_3)_2CO$ or $CDCl_3$ in the presence of tetramethylsilane (TMS) as an internal standard was used for the analysis of MC and MC-$[NH_2]_x$ copolymers. A YL-Clarity GPC system (YL instruments, Gyeonggi, Korea) equipped with a YL 9170 RI detector and three columns (Shodex K-802, K-803, and K-804 polystyrene gel columns) at 40 °C was used to determine the molecular weight distributions of copolymers. During the measurements, the flow rate of the $CHCl_3$ eluent was 1.0 mL/min.

2.3. Synthesis of MPEG-b-poly(ε-caprolactone) (MC)

MC copolymers with poly(ε-caprolactone) molecular weights of 2400 g/mol were prepared using MPEG (750 g/mol) as an initiator via a previously reported block copolymerization method [25].

2.4. Synthesis of MPEG-b-[poly(ε-caprolactone)-ran-poly(4-benzyloxy-ε-caprolactone)] (MC-OBn)

All glassware was heated in a vacuum and dried via flushing under a dry nitrogen stream. CL-OBn was prepared via a previously reported method [26]. We used the typical polymerization process for the synthesis of MC-$(OBn)_{10}$ with a CL/CL-OBn ratio of 90/10 using MPEG (750 g/mol) as an initiator. First, MPEG (0.94 g, 1.25 mmol) and toluene (30 mL) were added to a flask. Azeotropic distillation was performed to remove water from the MPEG and toluene. Next, toluene was removed via distillation under a dry nitrogen stream. CH_2Cl_2 (30 mL) was introduced to the MPEG with CL (2.47 g, 21.64 mmol) and CL-OBn (0.53 g, 2.4 mmol), followed by the addition of a 1.0 M solution of HCl in diethyl ether (1.5 mL) at room temperature. After 24 h, the mixture was poured into a mixture of *n*-hexane and EA (v/v = 40/10) to precipitate a copolymer. The precipitated copolymers were obtained from the supernatant by decantation, dissolved in CH_2Cl_2, and then filtered. The resulting copolymer solution was concentrated by rotary evaporation and dried in a vacuum, yielding a colorless copolymer (99%). MC-$(OBn)_{30}$ and MC-$(OBn)_{50}$ were prepared following the same procedures. The molecular weights and ratios of the MC-OBn segments in the copolymers were determined by comparing the intensity of the phenyl protons at δ = 7.2–7.4 ppm.

2.5. Synthesis of MPEG-b-[poly(ε-caprolactone)-ran-poly(4-hydoxyl-ε-caprolactone)] (MC-OH)

MC-$(OBn)_{10}$ (2.9 g, 1.1 mmol) was first dissolved in tetrahydrofuran (THF) anhydrous (30 mL). 10% w/w (4.5 g) of Pd/C [Palladium, 10 wt% (wet basis) on activated carbon (50% water w/w, Degussa type E101 NE/W)] was added to the MC-$(OBn)_{10}$ solution at room temperature under nitrogen flow, after which the mixture was stirred under a hydrogen atmosphere for 5 h. The reaction solution was then passed through a Celite filter. The organic phase was concentrated using a rotary evaporator and dried in a vacuum to obtain a colorless copolymer (94%).

2.6. Synthesis of MPEG-b-[poly(ε-caprolactone)-ran-poly(4-amine-ε-caprolactone)] (MC-NH_2)

For this step, MC-$(OH)_{10}$ (2.7 g, 1.07 mmol) and toluene (70 mL) were added to a flask. Azeotropic distillation was performed to remove the water. Under a dry nitrogen stream, the toluene was removed via distillation to achieve a final volume of 35 mL. Next, 4-nitrophenyl chloroformate (0.43 g, 4.28 mmol) and TEA (0.60 mL, 5.89 mmol) were added to an MC-$(OH)_{10}$ suspension at room temperature under constant nitrogen flow and stirred for 24 h. The reaction mixture was then poured into a mixture of *n*-hexane and ethyl ether (v/v = 4/1) to precipitate the copolymer. The obtained copolymer was then redissolved in CH_2Cl_2. The organic phase was concentrated by evaporation and dried in a vacuum to obtain a light yellowish copolymer [MC-(O-4-nitrophenyl formate)$_{10}$]. Next, MC-(*O*-4-nitrophenyl formate)$_{10}$ (2.60 g, 1.03 mmol) was dissolved in anhydrous THF (15 mL). Then, 1,4-butylene diamine (4.14 g, 46.96 mmol) in anhydrous THF (15 mL) was added at a 5 mL/min rate into the MC-(*O*-4-nitrophenyl formate)$_{10}$ solution and stirred for 24 h. The reaction mixture was then precipitated into a mixture of DW to remove 1,4-butylene diamine, which was separated from the supernatant by decantation. The organic phase was dried over anhydrous $MgSO_4$. The reaction mixture was then poured into a mixture of *n*-hexane and ethyl ether (v/v = 4/1) to precipitate the copolymer. The obtained copolymer was redissolved in CH_2Cl_2. The organic phase was concentrated by evaporation and dried in a vacuum to obtain a yellowish copolymer (MC-$(NH_2)_{10}$). MC-$(NH_2)_{30}$ and MC-$(NH_2)_{50}$ were prepared in the same way. The amine contents in MC-$(NH_2)_{10}$, MC-$(NH_2)_{30}$, and MC-$(NH_2)_{50}$ were measured by elemental analysis, ^1H NMR and ^{13}C NMR spectra, and the results were confirmed to be almost identical to the calculated target contents.

2.7. Determination of critical micelle concentration

The critical micelle concentration (CMC) of MC, MC-$(NH_2)_{10}$, MC-$(NH_2)_{30}$, and MC-$(NH_2)_{50}$ was determined using pyrene as a fluorescence probe. Pyrene solution in THF (1.2 mM) was solubilized in DW (1000 mL) and then THF was completely evaporated to prepare pyrene solution (1.2×10^{-6} M). MC, MC-$(NH_2)_{10}$, MC-$(NH_2)_{30}$, and MC-$(NH_2)_{50}$ were solubilized in DW to prepare stock solutions. The pyrene solution was added into the copolymer stock solution. A series of each concentration was prepared by dilution. All solutions were filtered by using 0.45 μm membrane filter and allowed to stand overnight at room temperature to equilibrate. The sizes of the resultant micelles were measured by electrophoretic light scattering (FPAR-1000, Otsuka, Japan). The micelle concentration varied from 1.0×10^{-6} to 1.0 mg/mL. The pyrene concentration in copolymer solution was 6×10^{-7} M. For the measurements of pyrene excitation spectra scan speed was set at 240 nm/min and, emission and excitation slit widths were set at 2.5 nm. For the excitation spectra, the emission wavelength was 335 nm. Fluorescence intensities of the pyrene entrapped in the micelle core were determined at 338 nm by an FP-8200 spectrofluorometer (JASCO, MD, USA) at room temperature.

2.8. Preparation of the AD emulsions

AD emulsions (F1–F5) were prepared in the formulations shown in Table S1. To prepare the oil phase, AD was first dissolved in ethanol. CCT oil, PEG-100 stearate, and MC or MC-$[NH_2]_x$ copolymers were added to the AD solution, after which the mixture was heated to 65 °C. For the preparation of the aqueous phase, glycerin, tetraglycol, and divinyldimethicone were dissolved in DW and heated to 65 °C. The oil and aqueous phases were then mixed at 65 °C and 25,000 rpm in a T-10 basic Ultra-Turrax Homogenizer (IKA Werke GmbH & Co. KG, Germany). After 5 min, silica silylate was added and mixed at 40 °C and 25,000 rpm. Finally, the AD emulsion was incubated at room temperature for 5 min.

2.9. Measurements of particle size and zeta potential

MC, MC-$[NH_2]_x$ copolymers or AD emulsions and CCT oil, PEG-100 stearate, glycerin, tetraglycol, and silica silicate solutions were prepared by dissolving the compounds in DW at 1 wt%. The particle sizes and zeta potentials of copolymer suspensions or AD emulsions were measured in triplicate via dynamic light scattering (ELSZ-1000; Otsuka Electronics, Osaka, Japan) at room temperature and reported as the mean and standard deviation.

To assess the stability of the AD emulsions, all emulsions were incubated at 4, 37, and 65 °C for 2 and 4 weeks. The stability of the AD emulsions was evaluated based on their clarity and phase separation. At 0, 2, and 4 weeks, 500 μL of the AD emulsions were dissolved in DW at a 1 wt% concentration and the particle sizes were measured three times by dynamic light scattering. All results converted by the Smoluchowski equation were reported as the mean and standard deviation.

2.10. Evaluation of the inflammatory effects of the AD emulsions using RAW 264.7 cells

RAW 264.7 (2×10^4 cells/well) were seeded in the lower chambers of 24-well Transwell plates (SPL Life Science, 0.4 μm pore size, Pocheon, Gyeonggi, Korea) and incubated for 1 d. Then, each formulation (200 μL) of AD emulsions was added to the upper chambers of the 24-well Transwell plates and cultured in DMEM supplemented with 10% FBS and 1% penicillin-streptomycin (PS) for one day at 37 °C in a humidified incubator containing 5% CO_2. At 1, 4, and 7 days, 100 μL of MTT (3-(4,5-dimethylthiazol-2-yl)-2,5-diphenyltetrazolium bromide) (Sigma-Aldrich Co., St Louis, MO, USA) solution (50 μL/mL in PBS) was added to the well plate and incubated at 37 °C for 4 h. Each plate was then gently mixed to form violet formazan. DMSO (500 μL) was added to each plate and shaken for 30 min. An aliquot from each well was then transferred to a 96-well plate (SPL Life Sciences, Gyeonggi-do, Korea). The absorbance of the solution was then measured at 590 nm using a microplate reader (E-max, Molecular Devices, Sunnyvale, CA, USA). All experiments were performed four times.

2.11. In vivo test – inflammatory animal modeling

All experimental protocols involving live animals were approved by the Institutional Animal Care and Use Committee (Approval No. 2014-0051) of the Ajou University School of Medicine. The *in vivo* experiments were conducted in accordance with guidelines approved by the Animal Ethics Committee for Care and Use of Laboratory Animals of the Ajou University Medical Center. All experiments were performed with six-week-old male nude mice (20–22 g) after anesthetizing them with 1:1 Zoletil-Rompun (60 μg/mL).

To induce acne inflammation, *Propionibacterium acnes* (P. acnes, ATCC 6919) bacteria were injected into the skin of nude mice (6 weeks old; Nara Bio, Seoul, Korea) at a concentration of 2×10^6 CFU/30 μL saline to obtain an experimental animal model.

In the early stages of infection, the inflammation caused by the bacteria resulted in severe swelling in the injection site. After approximately 6 h, the skin was stabilized and settled to a volume of 650–700 mm^3 and these mice were used as an acne inflammation model. The mice were divided into five groups (F1–F5), each of which was assigned a different test formulation (three animals per group); 200 μL of each formulation was applied to the induced acne inflammation area every 12 h for 7 days. The volume of acne vulgaris was determined by measuring the width, length, and height of the acne inflammation as follows: Volume (mm^3) = [length x $(width)^2$]/2.

2.12. Histological inflammatory animal analysis

The inflammatory animal models were treated as described in the previous subsection. After 1, 4, and 7 days, the experimental mice were euthanized and the skin tissue of the induced acne inflammation area was excised ($n = 3$ for each time point). The skin tissue was fixed with 10% formalin for 3 days. Afterward, the fixed tissues were embedded in paraffin and sectioned into 4-μm slices, dried for 6 h at room temperature, and placed in an oven at 60 °C for 2 h. The deparaffinized slides were washed twice with xylene and sequentially hydrated for 5 min in 95%, 70%, and 60% ethyl alcohol, then washed with DW.

For hematoxylin and eosin (H&E) staining, the slides were washed with running tap water and stained with hematoxylin (Sigma-Aldrich, St. Louis, MO, USA) for 3 min, then washed again with DW. The hematoxylin-stained slides were sequentially stained with 20% eosin (Sigma-Aldrich, St. Louis, MO, USA) for 3 min and washed with DW. Afterward, the stained slides were dried at room temperature for 3 h and then fixed and mounted with a mounting medium (Muto Pure Chemicals; Tokyo, Japan).

To identify decreases in skin thickness, the thickness of inflamed skin was measured at the inflammation site using H&E-stained samples with the ImageJ software (National Institutes of Health, Bethesda, MD, USA) and calculated with the following formula: *Decreasing skin thickness rate* (m/s) = [Δ (skin thickness)/Δ (time)]. All experiments were conducted at least in five randomly selected inflammation sites and the results are presented as mean ± standard deviation (SD).

For macrophage (ED1) staining, the paraffinized slides were deparaffinized as described above. The slides were then incubated for 10 min at 120–130 °C in a citrate buffer solution (Sigma-Aldrich). The slides were washed twice with PBS for 5 min, then washed with PBS-T (0.05% Tween 80 in PBS) for 10 min. Next, the slides were blocked in PBS containing 5% horse serum (HS; Gibco, Auckland, New Zealand) and 5% bovine serum albumin (BSA; Bovogen, Victoria, Australia) for 90 min at 37 °C. Afterward, the slides were incubated at 4 °C for 16 h with ED1 antibodies (mouse anti-rat CD68; Serotec, Oxford, UK) in antibody diluent (DAKO, Glostrup, Denmark; 1:1000). The specimens were then washed twice with PBS for 5 min, then with PBS-T for 10 min. The slides were subsequently incubated with a secondary antibody (goat anti-rat Alexa Fluor® 594, Invitrogen, USA; 1:200) for 3 h. The slides were washed again with PBS-T and mounted with Pro-Long Gold Antifade Reagent with DAPI. ED1-positive stained images were quantified using the ImageJ software at three random sites for each sample.

All of the stained slides were visualized using an Axio Imager A1 equipped with the Axiovision software (Rel. 4.8, Carl Zeiss Microimaging GmbH). ED1-positive stained images were quantified using the ImageJ software at three random sites for each sample and calculated with the following formula: *Decreasing rate of ED1-positive cell* (m/s) = [Δ (ED1-positive images)/Δ (time)]. All experiments were conducted at least in five randomly selected inflammation sites and the results are presented as mean ± SD.

2.13. Statistical analysis

Cytotoxicity data from RAW 264.7 cells were obtained from three independent experiments for each data point. The skin thicknesses were measured using H&E staining and the ED1-positive images were measured by ED1 staining in three independent experiments after 1, 4, and 7 days. The results were analyzed via one-way analysis of variance (ANOVA) with Bonferroni's post-hoc test using the SPSS 12.0 software (SPSS Inc., Chicago, IL, USA).

3. Results

3.1. Preparation and characterization of MC-$[NH_2]_x$ diblock copolymers

In previous works, we reported that polyester segments with a molecular weight below ~2000 g/mol and MPEG over 1000 g/mol were almost or completely water-soluble, whereas polyester segments with a molecular weight over ~2900 g/mol and MPEG below 1000 g/mol were only partially soluble in water [25–27]. Additionally, we found that main

poly(ε-caprolactone) segment of MC showed almost no/little degradation even after 6 weeks [28].

In this work, we designed diblock copolymers with an MPEG chain (M_n = 750 g/mol) and the molecular weight of the PCL segment was approximately 2400 g/mol with different pendant-group CL-OBn contents, which was achieved by varying the ratios of CL and CL-OBn.

First, MC-$[OBn]_x$ was prepared via the ring-opening polymerization of the CL and CL-OBn monomers with benzyl pendant-group contents of 10, 30, and 50 mol% (Fig. 2 and Tables S2). The ratios of CL and CL-OBn in the MC-$[OBn]_x$ copolymers were determined based on the proton or carbon integration ratios in the ^{1}H NMR or ^{13}C NMR spectra (Figs S1-S4). The calculated benzyl segment ratios of MC-$[OBn]_x$ agreed well with the expected values. The benzyl group from the obtained MC-$[OBn]_x$ was developed using Pd/C to obtain MC-$[OH]_x$. The signal of the phenyl group of the MC-$[OBn]_x$ diblock copolymers at 7.2–7.4 ppm (assigned to the phenyl groups) was no longer detected in MC-$[OH]_x$. Finally, MC-$[NH_2]_x$ was obtained via the reaction of MC-$[OH]_x$ with 1,4-diaminobutane. MC-$[NH_2]_x$ exhibited ^{1}H NMR peaks characteristic of NH_2. The amounts of NH_2 in the MC-$[NH_2]_x$ copolymers were determined by the ^{1}H NMR or ^{13}C NMR peaks and elemental analysis, which almost agreed with the target contents of the NH_2 pendant group (Table S3). Collectively, these findings indicated that the NH_2 groups were modified at the pendant position on the MC segment.

As a control diblock copolymer, MC diblock copolymers were prepared via ring-opening polymerization of the CL monomer alone using the terminal alcohol of MPEG as the initiator.

3.2. Solution properties of MC and MC-$[NH_2]_x$

MC and MC-$[NH_2]_x$ copolymers were dissolved in DW at a 1 wt% concentration (Fig. 3a). Current measurements indicated that the MC solution possessed an anionic zeta potential of −5 mV although there was no anionic moiety in the MC copolymer, which was likely due to the electronegativity of the carbonyl group in the poly(ε-caprolactone) segment and oxygen groups in the MPEG segment. The MC-$(NH_2)_{10}$ solution exhibited a positive potential of 10.3 mV. Afterward, the charge potential of MC-$(NH_2)_{30}$ of 15.5 mV and MC-$(NH_2)_{50}$ of 23.0 mV gradually increased as the amine contents in MC-$[NH_2]_x$ increased.

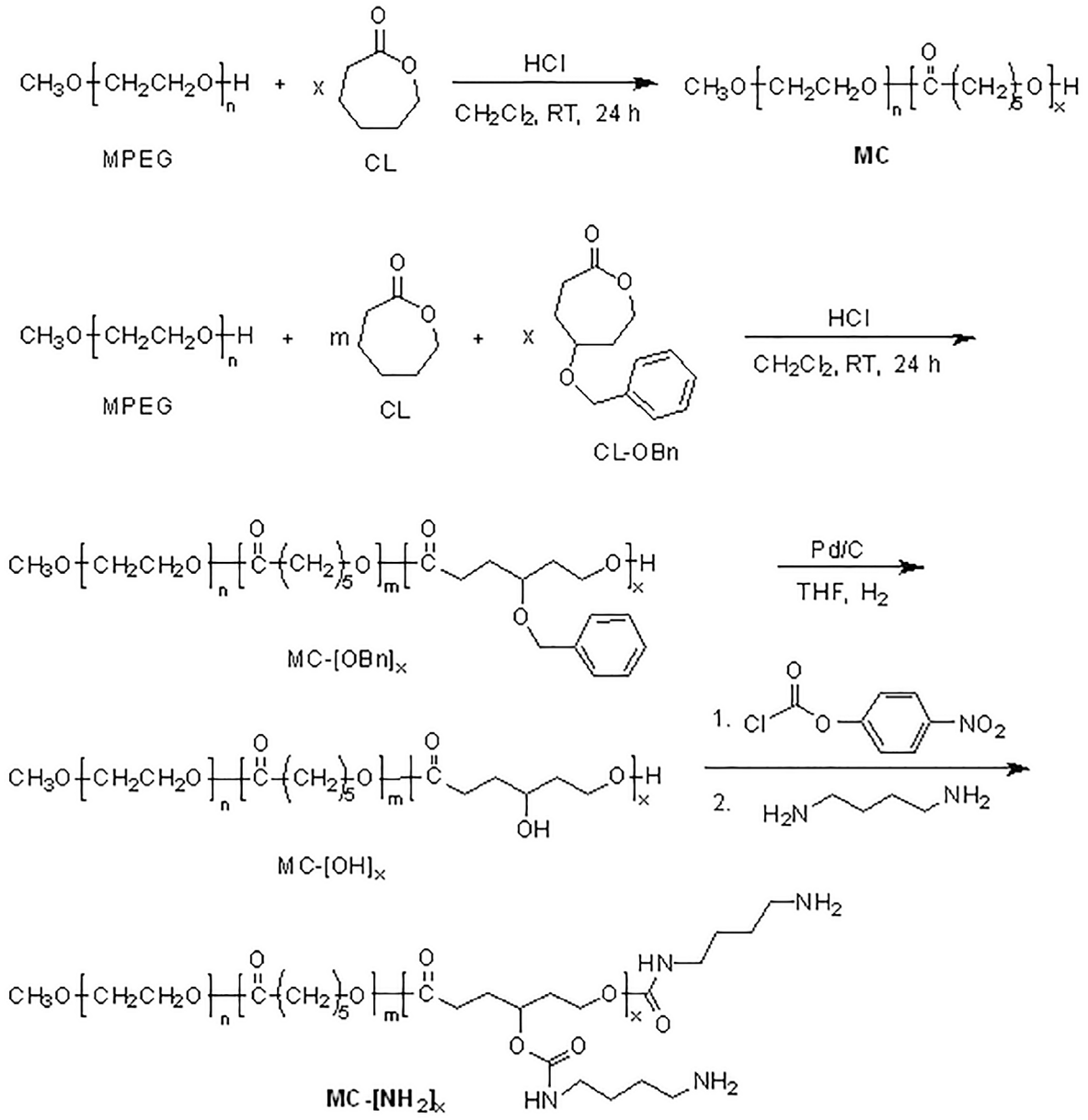

Fig. 2. Preparation of the anionic MC and cationic MC-$[NH_2]_x$ copolymer.

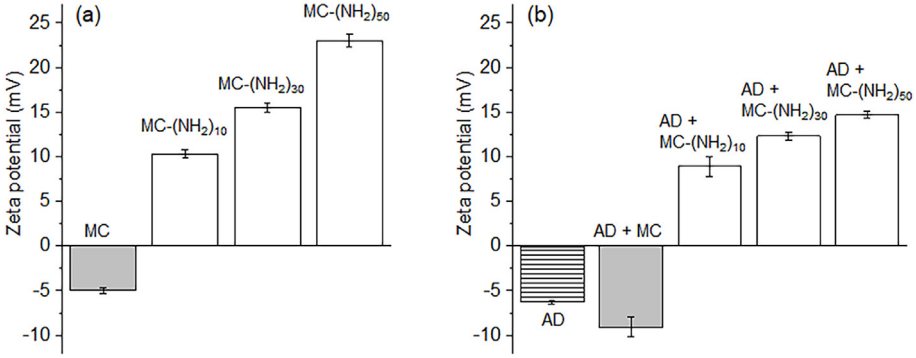

Fig. 3. Zeta potential of (a) the anionic MC and cationic MC-$[NH_2]_x$ copolymer solutions and (b) AD alone and solution mixtures of AD with anionic MC and cationic MC-$[NH_2]_x$.

Additionally, MC and MC-$[NH_2]_x$ copolymers were solubilized in DW to observe the formation of micelles. A slight blue color was observed, indicating the formation of MC and MC-$[NH_2]_x$ micelles. The MC micelles were 646 nm in size, whereas the MC-$(NH_2)_{10}$, MC-$(NH_2)_{30}$, and MC-$(NH_2)_{50}$ micelles were 477, 403, and 322 nm, respectively. These results indicated that the micelle sizes were likely affected by the variations in the NH_2 pendant group ratios of MC-$[NH_2]_x$.

Next, the CMC of the resulting copolymer micelles were determined to compare the nature of NH_2 pendant group ratios (Fig S5). The CMC values of the MC and MC-$[NH_2]_x$ are in the range of $1.0 \times 10^{-3} - 3.5 \times 10^{-3}$ mg/mL. The CMC increased in the following order: MC < MC-$(NH_2)_{10}$ < MC-$(NH_2)_{30}$ < MC-$(NH_2)_{50}$. This sequence indicates that the copolymers with more NH_2 pendant group formed micelles less easily than those with lower NH_2 pendant group. These findings thus suggest that the CMC increases as the NH_2 pendant group increases.

Next, MC and MC-$[NH_2]_x$ copolymers were mixed with AD, after which the electrostatic properties of these mixtures (i.e., AD-MC and AD-MC-$[NH_2]_x$) were measured. AD alone exhibited a negative zeta potential of −6.3 mV. The net zeta potential of AD-MC increased to more negative values (−9.1 mV) as a result of mixing AD with MC, the latter of which also had a negative zeta potential (−5 mV).

In contrast, AD-MC-$[NH_2]_x$ exhibited positive zeta potentials due to the neutralization of the zeta potential between the cationic MC-$[NH_2]_x$ and negative AD. The net zeta potential of AD-MC-$[NH_2]_{10}$ was 8.9 mV and increased to more positive values when the amine contents in MC-$[NH_2]_x$ increased.

Our results confirmed that the arithmetic calculation of the zeta potentials of cationic MC-$[NH_2]_x$ electrolytes and anionic AD electrolytes were in good agreement with the expected electrostatic properties. Furthermore, these findings suggested the occurrence of electrostatic interactions between cationic MC-$[NH_2]_x$ electrolytes and anionic AD electrolytes.

3.3. *Preparation and characterization of AD-loaded MC or MC-$[NH_2]_x$ emulsions*

Various emulsion formulations were prepared with several compositions of AD with MC or MC-$[NH_2]_x$ as an electrostatic emulsifier (Table S1). First, AD was dissolved in ethanol, followed by CCT oil, PEG-100 stearate, and MC or MC-NH_2 to prepare the oil phase. The aqueous phases were prepared using glycerin and tetraglycol with divinyldimethicone as a solubilizer. Then, the oil and aqueous phases were mixed with a homogenizer to prepare the emulsions.

All emulsions produced a uniform dispersion of AD in isotropic mixtures of the oil and aqueous phases (Fig. 4a and Fig S6). This indicated that the AD emulsions (F1–F5) can be formed as isotropic mixtures of the oil and aqueous phases with different MC or MC-$[NH_2]_x$. Finally, silica silylate was added to control the viscosity of the AD emulsions. The prepared AD emulsions showed visually white dispersion of AD,

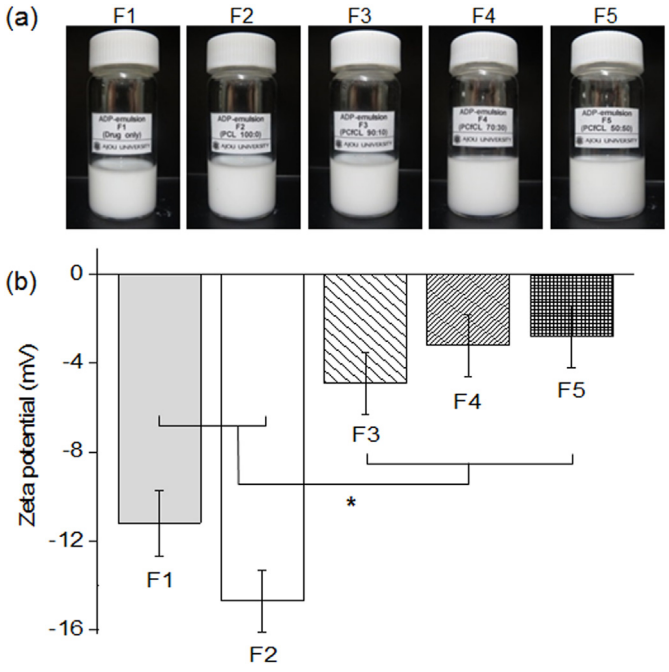

Fig. 4. (a) Images and (b) zeta potential of the emulsion containing AD only (F1), AD emulsion with MC (F2), and AD emulsion with MC-$[NH_2]_x$ (F3, F4, and F5) (*$p < 0.05$).

indicating that AD was successfully incorporated into the emulsions. The prepared AD emulsions (F1–F5) were used in downstream characterizations and further skin studies.

Next, the electrostatic properties of the AD emulsions were measured. All AD emulsions showed negative zeta potentials because the zeta potentials of CCT oil, PEG-100 stearate, glycerin, tetraglycol, and silica silicate were all negative (Fig S7).

The net zeta potentials of the emulsion containing only AD (F1: 11.2 mV) were higher than that of AD itself (−6.3 mV) due to the negative zeta potentials of CCT oil, PEG-100 stearate, glycerin, tetraglycol, and silica silicate. The F2 AD emulsion exhibited a more negative value (−14.7 mV) due to the incorporation of the anionic MC compared with the negative zeta potentials of the emulsion containing only AD (−11.2 mV) and the original negative zeta potential of anionic MC (−5 mV).

Although the F3–F5 AD emulsions showed negative net zeta potentials, they however exhibited a reduction in negative zeta potential due to the neutralization of the zeta potential of cationic MC-$[NH_2]_x$. These results indicated that the electrostatic properties between the negative zeta potentials of AD and the positive zeta potential of MC-$[NH_2]_x$ were in good agreement with our calculations. Furthermore, these findings

indicated that the net zeta potentials of the F3–F5 AD emulsions resulted from the electrostatic interaction between cationic MC-$[NH_2]_x$ and anionic electrolyte AD drugs even after the preparation of the AD emulsions.

3.4. Stability of the AD emulsions

The next objective of this study was to develop stable AD emulsions. The stability of an emulsion is a key characteristic of safe and effective drug delivery formulations. Therefore, stability of the AD emulsions was examined at 4, 37, and 65 °C for 2 and 4 weeks (Fig. 5).

All AD emulsions at 4 °C exhibited no marked change in appearance and little size changes up to 4 weeks compared to the corresponding initial formulation. However, at 37 °C, all AD emulsions exhibited a slight increase in particle sizes at 2 weeks but a significant increase in particle sizes compared to the corresponding initial AD emulsions on week 0. Furthermore, all AD emulsions exhibited an increase in particle sizes at 2 and 4 weeks. Additionally, two separate particle sizes were observed at the beginning of the experiments, which collapsed after the formation of large particles, at which point the precipitated particles were barely discernible after 2 weeks. Particularly, the F2 and F3 emulsions prepared with anionic MC or cationic MC-$[NH_2]_x$ with low cationic charge potentials showed large particles and particle disintegration even at 2 weeks or 4 weeks, respectively. Generally, the AD emulsions (F4 and F5) exhibited relatively small changes in particle sizes without particle segregation.

Collectively, our findings indicated that the F4 and F5 AD emulsions were highly stable in the short-term studies at elevated temperatures and for at least 1 month at 37 °C. In turn, these findings suggest that cationic MC-$[NH_2]_{30}$ and MC-$[NH_2]_{50}$ formed more stable AD emulsions than anionic MC.

3.5. Viability of RAW 264.7 cells on AD emulsions

All AD emulsions prepared in this work were tested on the acne inflammation model. Therefore, the effect of the AD emulsions on the viability of RAW 264.7 cells was evaluated and a no-drug treatment was included as a control. All AD emulsions were able to diffuse from the upper chamber to the bottom chamber to contact the RAW 264.7.

The viability of RAW 264.7 cells was evaluated at 1, 4, and 7 days (Fig. 6). Untreated RAW 264.7 control cells showed a rapid increase in viability as a function of culture time. In the groups treated with the AD emulsions, the viability of the RAW 264.7 cells decreased to approximately 50%–60% compared to the control on day one due to the diffusion of the AD in the AD emulsions from the upper chamber to the bottom chamber, indicating that AD has an inhibitory effect on the viability of RAW 264.7 cells. After four and seven days, all AD emulsions decreased RAW 264.7 cell viability to below 2% of that of the corresponding control cells. This indicated that the AD released from the AD emulsions almost completely inhibited the proliferation of RAW 264.7 cells over the experimental period.

3.6. In vivo evaluation of the therapeutic properties of the emulsions against acne inflammation

Prior to treating the animals with acne inflammation, AD emulsions were first administered on normal non-inflamed skin. The AD emulsions did not cause any visible redness or swelling on normal skin, suggesting that the AD emulsions had no adverse effects on the skin.

Next, the skins of the animals were treated with a bacterial injection to induce acne inflammation. The skins were severely swelled to a volume of 650–700 mm^3, and the swelled skin exhibited purulent acne in the form of pus. The skin morphology of the inflamed area was inspected and the change in volume was measured (Fig. 7).

Upon inducing inflammation, a non-treatment group was used as a control. The volume of the acne inflammation area decreased from its initial size over the course of seven days. However, the inflammation became progressively more severe, which was accompanied by the bursting of pus-filled abscesses and an increase in the peeled skin area with time. This inflammatory cascade typically led to the formation of inflammatory acne lesions, including papules, infected pustules, or nodules. The inflammatory acne without treatment exhibited a degradation of the deeper layers of the dermis and subcutaneous tissue, resulting in the formation of deep nodules.

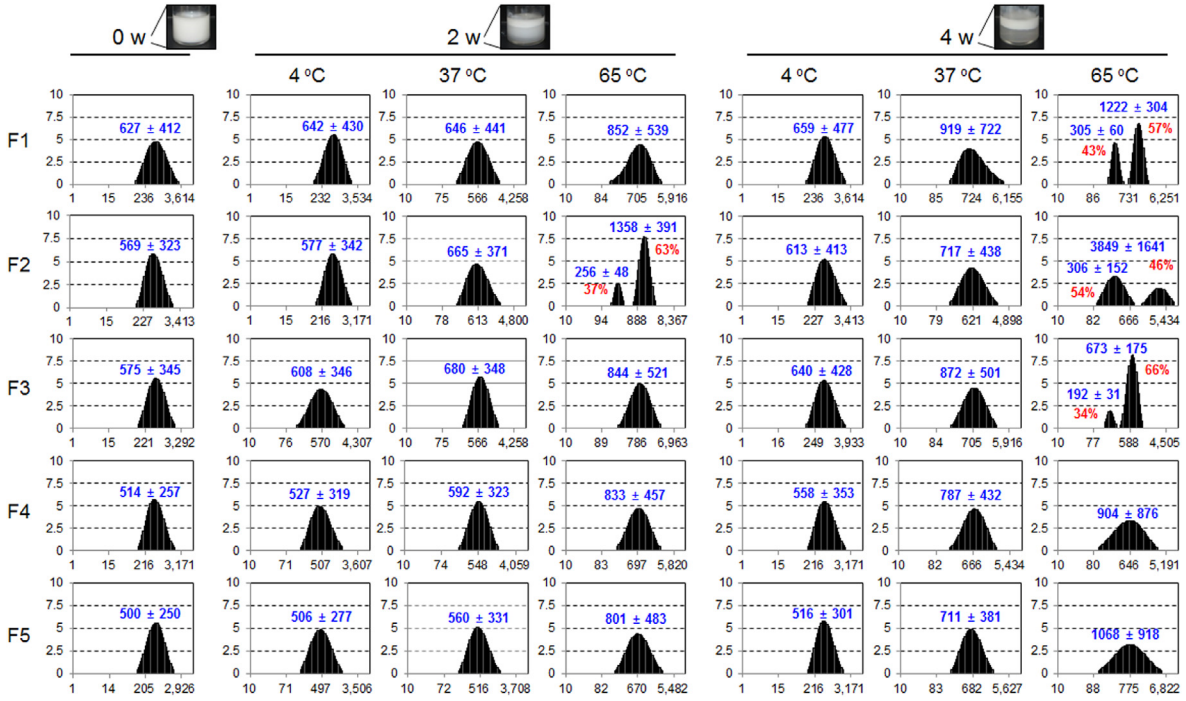

Fig. 5. Changes in particle size of the AD only emulsion (F1), AD emulsion with MC (F2), and AD emulsions with MC-$[NH_2]_x$ (F3, F4, and F5) at 4, 37, and 65 °C for 4 weeks.

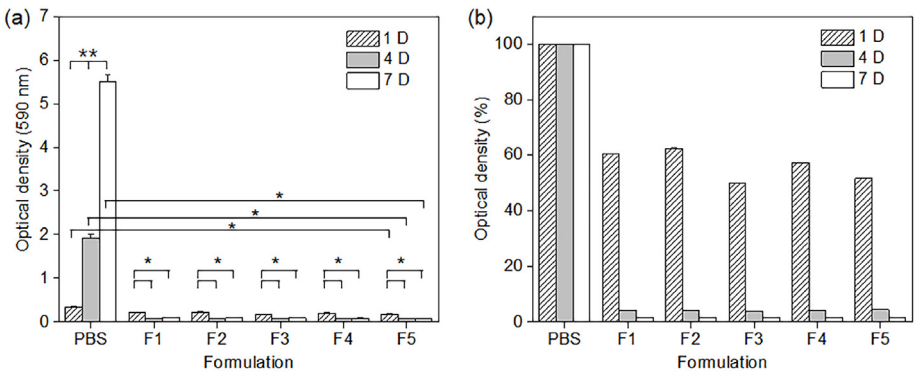

Fig. 6. (a) Viability of Raw 264.7 cells measured by the MTT assay at 1, 4, and 7 days and (b) relative ratios by proportional calculation of each formulation at the corresponding days after treatment with AD emulsions (F1–F5) compared with the PBS-treated group (as measured by the (a) results of the MTT assay) (*$p < 0.05$, **$p < 0.005$).

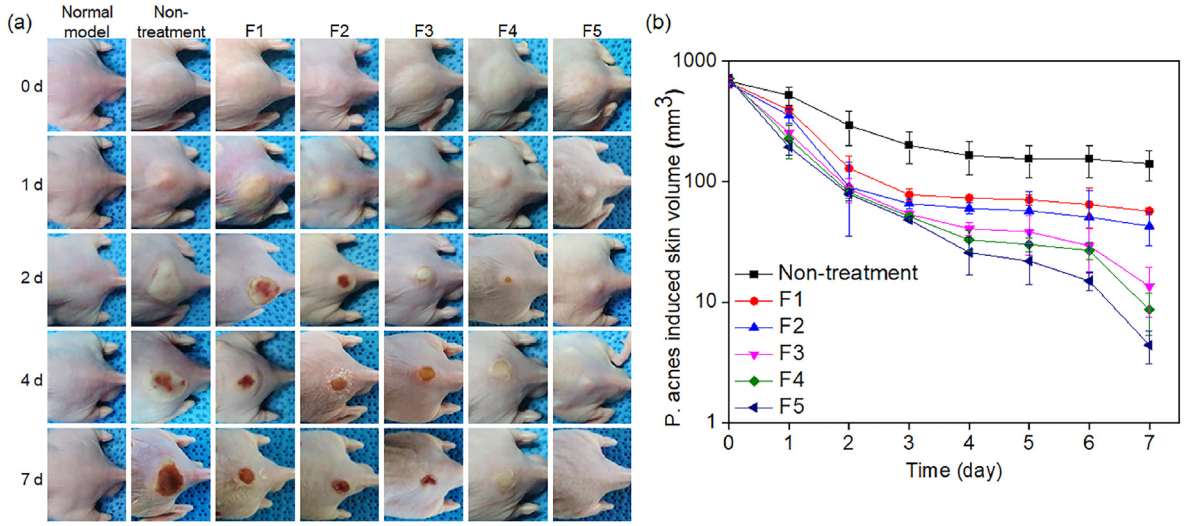

Fig. 7. (a) Images of skins of nude mice and acne-induced skin areas after non-treatment and AD emulsion treatment (F1–F5) of nude mice with acne vulgaris, and (b) acne volume for each treatment as a function of time.

After the administration of the AD emulsions, skin morphology and acne inflammation volume were assessed to evaluate the *in vivo* healing effects. The animals treated with the F1, F2, and F3 emulsions exhibited severe inflammation and bursting pustules. However, the peeled skin area decreased progressively to 9%, 7%, and 21% in each of these treatments, respectively. In contrast, the F4 group exhibited a reduction in inflammation accompanied by only slight skin peeling at 2 days. Additionally, very little pus and peeled skin were observed at 4 days and the skin appeared almost normal at 7 days. These anti-inflammatory effects demonstrated that the emulsified AD was effective against acne vulgaris.

Furthermore, the F5 emulsion group exhibited less inflammation and almost no skin damage. Additionally, the volume of the acne inflammation decreased to only 0.6% after 7 days compared with the initial wound area. Therefore, the F5 emulsion exhibited the best and quickest therapeutic effects. These findings suggested that the formulation of the F5 emulsion remarkably enhanced the penetration of AD across the skin by delivering AD to the dermis through the epidermis via the electrostatic attraction between MC-$[NH_2]_{50}$ and the negatively charged stratum corneum.

3.7. *In vivo* assessment of acne inflammation healing via histological analysis

The healing of acne inflammation was evaluated using H&E-stained histological images for the treatment groups sampled 1, 4, and 7 days after administration of the AD emulsions, as well as the non-treated group (Fig. 8). The H&E-stained histological images for normal skin clearly showed the epidermis, dermis, and subcutaneous tissue.

The skin of the non-treated group showed considerable deformation with inflammation in the skin layer and a circular configuration due to the purulent acne at 1 and 4 days. Circular structures (i.e., pustules) were observed at 7 days even though the stained image of the purulent acne showed a size reduction. These symptoms eventually led to scar formation. On day 1, all AD emulsions resulted in the inflammation of the skin layer and purulent acne similar to the non-treated group. At four days, the treatment groups exhibited the following order based on the size of the purulent acne: F5 > F4 > F3 > F2 > F1 > non-treatment.

The thickness of the normal skin increased slightly over time (4.39×10^{-10}). In contrast, the skin thickness in both the non-treated and the AD emulsion-treated groups (F1–F5) exhibited a decreasing constant rate

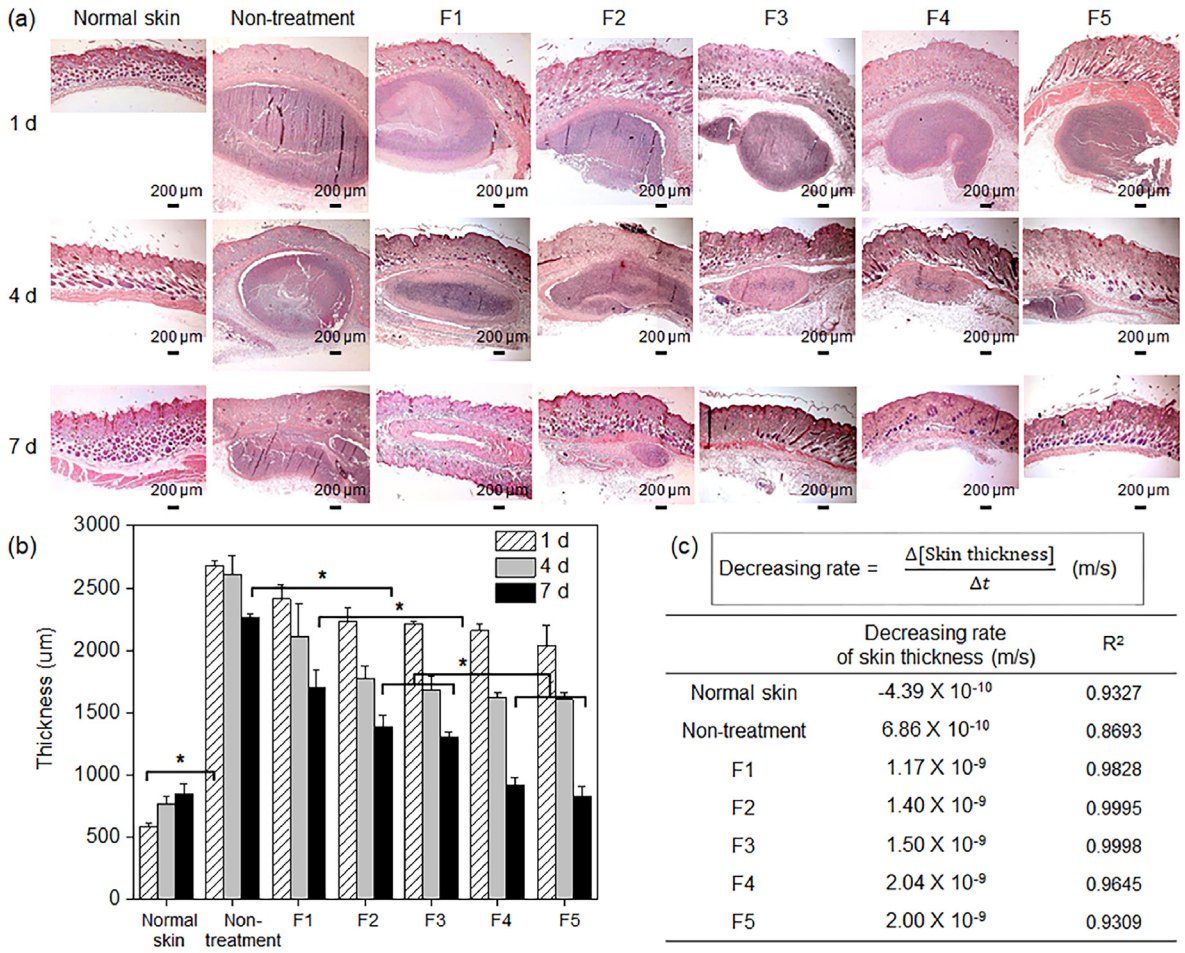

	Decreasing rate of skin thickness (m/s)	R^2
Normal skin	-4.39×10^{-10}	0.9327
Non-treatment	6.86×10^{-10}	0.8693
F1	1.17×10^{-9}	0.9828
F2	1.40×10^{-9}	0.9995
F3	1.50×10^{-9}	0.9998
F4	2.04×10^{-9}	0.9645
F5	2.00×10^{-9}	0.9309

Fig. 8. (a) H&E staining, (b) quantitative analysis of skin thickness (determined by H&E staining images) (*$p < 0.001$), and (c) decreasing rate constant of skin thickness after non-treatment and treatment with AD emulsions (F1–F5) as a function of time.

with time. The non-treated and AD emulsion-treated animals (F1–F5) exhibited skin thickness slopes of -6.86×10^{-10}, -1.17×10^{-9}, -1.40×10^{-9}, -1.50×10^{-9}, -2.04×10^{-9}, and -2.00×10^{-9} m/s over time, respectively. These slopes confirmed that the F5 AD emulsion decreased skin thickness by 2.9, 1.7, and 1.4 times, respectively, compared to non-treated group and the other evaluated AD emulsions [F1 (AD alone) and F2 (anionic MC)].

The AD emulsion-treated animals (F1–F5) exhibited some epidermal regeneration after 4 and 7 days. On the other hand, after 4 and 7 days, the skins of the F4 and F5 groups exhibited a relatively organized epidermis structure. Particularly, significant mature granulation tissue in the epidermis was evident in the skins due to the fast skin healing of the F5 AD emulsion-treated group.

Inflammation, especially the type that is mediated by macrophages, plays a critical role in the skin healing process. Thus, we further characterized macrophage staining (ED1: red) to determine the extent of the inflammatory response after 1, 4, and 7 weeks (Fig. 9). In the non-treated group, red and blue fluorescent signals were evident at all three measurement times. Although the non-treated group was characterized by a progressive decrease in macrophages with time, high numbers of macrophages were still observed after 4 and 7 days.

All AD emulsion-treated groups showed high numbers of macrophages on day 1, which decreased gradually with time. The stained skins in the F1, F2, and F3 groups exhibited 15%–19% ED1-positive staining cells on day 1, which progressively decreased to 11%–12% with time.

In contrast, groups F4 and F5 exhibited high numbers of ED1-positive staining cells on day 1 but had fewer ED1-positive staining cells than the F1, F2, F3, and non-treated groups after 1, 4, and 7 days. Furthermore, the F4 and F5 treatments substantially suppressed the inflammatory response. Particularly, the F5 group exhibited the lowest number of macrophages (below 2%) at seven days compared to the other emulsion-treated groups.

The number of ED1-positive macrophages was plotted as a function of time and calculated as a constant rate. All experimental groups exhibited a decreasing constant rate of macrophage expression. Particularly, the macrophage numbers of the F5 group were 2.9 and 2.3 times less than those of the non-treated and F1 groups. Therefore, our findings demonstrated that the F5 treatment strongly suppressed the inflammatory response and the AD in the emulsions modulated macrophage expression during the skin healing process. Collectively, these results demonstrated that the F5 AD emulsion formed by strong electrostatic attraction had better immunomodulatory effects for healing acne inflammation.

4. Discussion

The topical application of AD (i.e., a *trans*-retinoic acid) is commonly used to treat severe acne vulgaris. AD treatment, however, presents many difficulties due to its negative charge and poor stability. Several different approaches for AD delivery to the dermis through the epidermis have been previously investigated [21–24].

In recent years, several attempts have been made to develop AD-based topical treatments against acne vulgaris. These approaches have

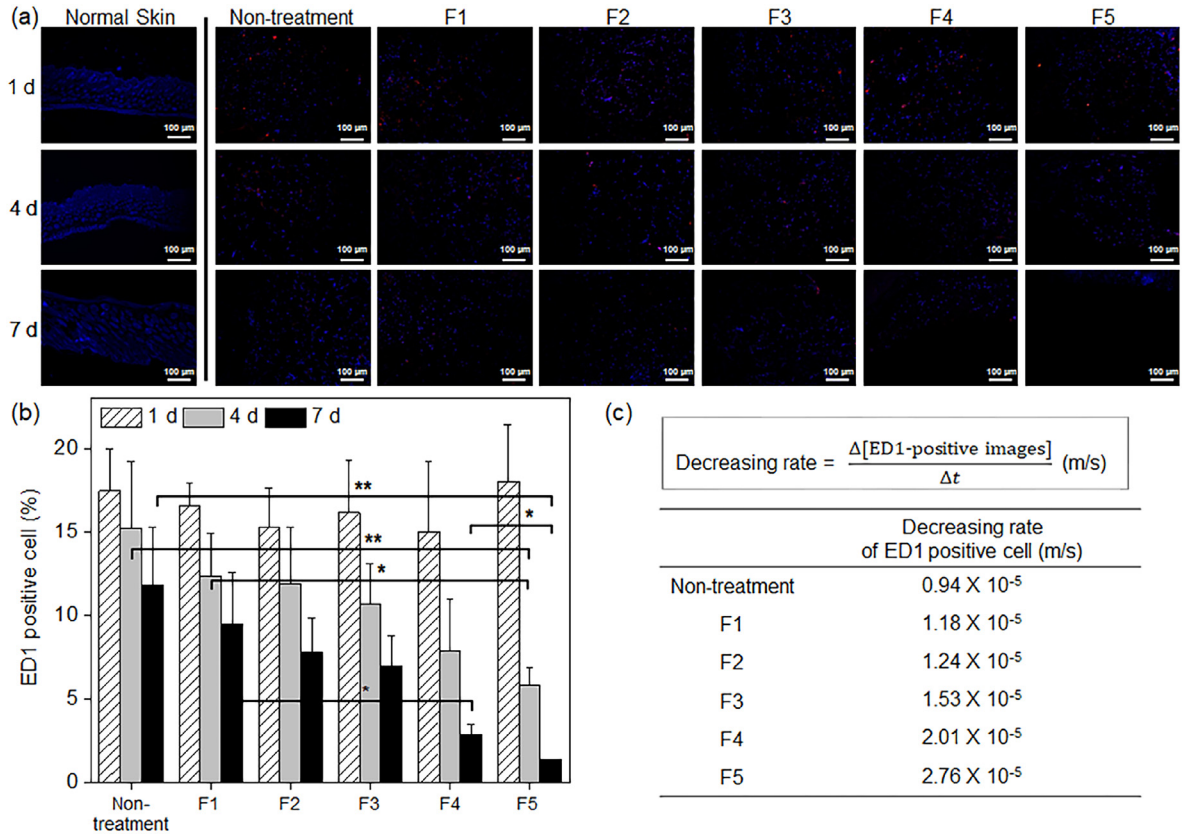

	Decreasing rate of ED1 positive cell (m/s)
Non-treatment	0.94 X 10^{-5}
F1	1.18 X 10^{-5}
F2	1.24 X 10^{-5}
F3	1.53 X 10^{-5}
F4	2.01 X 10^{-5}
F5	2.76 X 10^{-5}

Fig. 9. (a) ED1 staining, (b) quantitative analysis of ED1 positive cells (determined by ED1 staining images) (*$p < 0.05$, **$p < 0.01$), and (c) decreasing rate constant of ED1-positive cells after non-treatment and treatment with AD emulsions (F1–F5) as a function of time.

focused on formulating AD ointments with emulsifiers and lipids to improve solubility, thus allowing for the delivery of AD to the dermis through the epidermis.

Here, we presented a new approach to address some issues of anionic AD by comparing AD emulsions that were electrostatically optimized using anionic MC and cationic MC-$[NH_2]_x$ as electrostatic emulsifiers. We successfully prepared a cationic MC-$[NH_2]_x$ emulsifier with different cationic charge ratios via sequential modification reactions after living polymerization [23]. The zeta potentials of the mixtures of cationic MC-$[NH_2]_x$ electrolytes and anionic AD electrolytes were almost identical to our calculated estimations [28,29].

Our findings suggested that the cationic MC-$[NH_2]_x$ electrolytes as a cationic emulsifier can facilitate the solubilization of anionic AD. Here, we successfully prepared AD emulsions whose net charges could be precisely controlled by adjusting the ratios between cationic MC-$[NH_2]_x$ electrolytes and anionic AD. Therefore, cationic MC-$[NH_2]_x$ electrolytes were used to optimize the formulation of AD emulsions.

Furthermore, the present study assessed the stability and efficacy of the AD emulsions. We found that the AD emulsions prepared with high cationic MC-$[NH_2]_x$ charge were highly stable in the short-term studies at elevated temperatures and for at least 1 month at 37 °C. Meanwhile, because poly(ε-caprolactone) segment of MC showed almost no/little degradation even after 6 weeks in previous work [27,28], it is conjectured that MC-$[NH_2]_x$ in AD emulsions maintained a stable structure even at current elevated temperatures. This suggested that electrostatically optimized AD emulsions possess stable thermodynamic properties for a relatively long time because their high cationic charge can form a more stable AD emulsion via the formation of electrostatic interactions with the anionic AD.

Furthermore, the AD emulsions prepared in this work do not have the problems of flocculation, coalescence, or sedimentation, thus ensuring better stability and longer shelf-life. Additionally, the AD emulsions did not cause any side effects on normal noninflammatory skin.

Next, we evaluated the ability of the AD emulsions containing the cationic MC-$[NH_2]_x$ emulsifier to deliver AD into the dermis through the epidermis via topical application. The lipid lamellae of the stratum corneum contain a high proportion of negatively charged lipids, and therefore the skin acts as a negatively charged membrane [30,31]. Thus, the positively charged MC-$[NH_2]_x$ emulsifier may facilitate the absorption of AD through the skin membrane.

We also found that the AD emulsions presented some beneficial properties for the topical treatment of acne vulgaris through the delivery of anionic AD into the dermis through the epidermis. Particularly, the AD emulsion prepared with the cationic MC-$[NH_2]_x$ emulsifier showed the best therapeutic effect against acne vulgaris. This phenomenon indicated that the AD emulsions remarkably enhance the penetration of AD across the skin, which was likely because the negatively charged stratum corneum favors the electrostatic attraction with the cationic emulsifier.

A similar phenomenon for the skin permeation has been observed by other investigators [32]. In the Higuchi, Ritger–Peppas, and Weibull equations [33,34], the skin permeation data were fitted to first-order. The skin healing by AD emulsions were fitted to first-order. In all cases of AD emulsions nice fittings were obtained (R^2 range 0.938–0.999), but R^2 of non-treatment was 0.869. This suggests that skin permeation of AD emulsions with the cationic MC-$[NH_2]_x$ remarkably enhance the penetration of entrapped AD across the skin. Additionally, this suggests the skin permeation of the AD emulsions prepared with MC-$[NH_2]_{30}$ and MC-$[NH_2]_{50}$ with high cationic charge would likely be substantially higher than that of other emulsions.

The onset of acne vulgaris is invariably accompanied by severe inflammation. Inflammation, especially the type that is mediated by macrophages, plays a critical role in the wound healing process. In

general, inflammation occurs as a series of processes to regenerate tissue against changes induced by physicochemical stimuli or bacterial infection. This results in the expression of macrophages and mast cells, which play an important role in the early stage of infection, followed by an aggravation of the inflammatory response through related biological processes.

In this work, all AD emulsions significantly inhibited RAW 264.7 cells. Additional *in vivo* evaluation of macrophage staining (ED1) was conducted to determine the extent of the inflammatory response. Although the non-treated group was characterized by a decrease in macrophages, all AD emulsions showed a gradual and fast decrease in macrophage expression with increased treatment time. This indicated that the AD emulsions effectively inhibited inflammation by acting on the inflammation-associated pathways that govern the onset of acne vulgaris. This result is consistent with the general report that topical AD administration significantly improved inflammatory lesions resulting from acne vulgaris. Furthermore, the AD emulsions with MC-$[NH_2]_{30}$ and MC-$[NH_2]_{50}$ with high cationic charge remarkably inhibited macrophage expression. Therefore, we concluded that the AD emulsions had a good therapeutic effect on acne vulgaris.

5. Conclusion

Our findings demonstrated the effective penetration of AD in AD emulsions with differently charged emulsifiers across the skin, which has a high proportion of negative charges. It was also confirmed that the formulated AD emulsions did not damage normal non-inflamed skin. Moreover, the AD emulsion prepared with the cationic emulsifier with high cationic charge potential provided an efficient therapeutic effect for the treatment of acne vulgaris. Although additional studies on large animals are needed to confirm the therapeutic efficacy of the emulsions formulated herein, our findings demonstrated that these AD emulsions have the potential to improve the therapeutic efficacy of acne vulgaris treatments, as well as patient compliance. A more detailed comparison study on the therapeutic efficacy of acne vulgaris treatments using commercial AD products (gels, creams) is planned as future work.

Author statement

Conceptualization, Y.B.J., H.Y.L. and M.S.K.; Formal analysis, H.Y.L., Y.B.J., S.L., Y.H.K., and J.H.K.; data Formal analysis, H.Y.L., Y.B.J., S.L., Y.H.K., K.N., J.H.K. and M.S.K.; Methodology, H.Y.L., Y.B.J., S.L., Y.H.K., K.N., J.H.K. and S.C.; Validation, H.Y.L., Y.B.J., S.L., Y.H.K., and M.S.K.; Visualization, H.Y.L. and Y.B.J.; Funding acquisition, S.C., and M.S.K.; Project administration, S.C., and M.S.K.; Supervision, M.S.K.; writing—original draft, H.Y.L.; writing—review and editing, M.S.K. All authors have read and agreed to the published version of the manuscript.

Declaration of competing interest

The authors declare that they have no known competing financial interests or personal relationships that could have appeared to influence the work reported in this paper.

Acknowledgments

This study was supported by the National Research Foundation of Korea (NRF) grants, Creative Materials Discovery Program (2019M3D1A1078938) and Priority Research Centers Program (2019R1A6A1A11051471).

Appendix A. Supplementary data

Supplementary data to this article can be found online at https://doi.org/10.1016/j.mtbio.2022.100339.

References

[1] H.H. Tan, Antibacterial therapy for acne: a guide to selection and use of systemic agents, Am. J. Clin. Dermatol. 4 (5) (2003) 307–314.
[2] D.D. Nguyen, L. Luo, J. Lai, Thermogels containing sulfated hyaluronan as novel topical therapeutics for treatment of ocular surface inflammation, Mater, Today Bio 13 (2022), 100183.
[3] G. Han, J.J. Wu, J.Q. Del Rosso, Use of topical tazarotene for the treatment of acne vulgaris in pregnancy: a literature review, J. Clin. Aesthet. Dermatol. 13 (9) (2020) E59–E65.
[4] B. Stuart, E. Maund, C. Wilcox, K. Sridharan, G. Sivaramakrishnan, C. Regas, D. Newell, I. Soulsby, K.F. Tang, A.Y. Finlay, H.C. Bucher, P. Little, A.M. Layton, M. Santer, Topical preparations for the treatment of mild-to-moderate acne vulgaris: systematic review and network meta-analysis, Br. J. Dermatol. 185 (3) (2021) 512–525.
[5] I. Aslam, A. Fleischer, S. Feldman, Emerging drugs for the treatment of acne, Expet Opin. Emerg. Drugs 20 (1) (2015) 91–101.
[6] A. Rusu, C. Tanase, G.A. Pascu, N. Todoran, Recent advances regarding the therapeutic potential of adapalene, Pharmaceuticals 13 (9) (2020) 217.
[7] M. Chivot, Retinoid therapy for acne. a comparative review, Am. J. Clin. Dermatol. 6 (1) (2005) 13–19.
[8] N. Tiwari, E.R. Osorio-Blanco, A. Sonzogni, D. Esporrín-Ubieto, H. Wang, M. Calderón, Nanocarriers for skin applications: where do we stand? Angew. Chem., Int. Ed. Engl. 61 (3) (2022), e202107960.
[9] A.J. Paredes, F. Volpe-Zanutto, L.K. Vora, I.A. Tekko, A.D. Permana, C.J. Picco, H.O. McCarthy, R.F. Donnelly, Systemic delivery of tenofovir alafenamide using dissolving and implantable microneedle patches, Mater. Today Bio 13 (2022), 100217.
[10] Y. Li, J. Yang, Y. Zheng, R. Ye, B. Liu, Y. Huang, W. Zhou, L. Jiang, Iontophoresis-driven porous microneedle array patch for active transdermal drug delivery, Acta Biomater. 121 (2021) 349–358.
[11] L. Barnum, J. Quint, H. Derakhshandeh, M. Samandari, F. Aghabaglou, A. Farzin, L. Abbasi, S. Bencherif, A. Memic, P. Mostafalu, A. Tamayol, 3D-printed hydrogel-filled microneedle arrays, Adv. Healthc. Mater. 10 (13) (2021), e2001922.
[12] S. Kusama, K. Sato, Y. Matsui, N. Kimura, H. Abe, S. Yoshida, M. Nishizawa, Transdermal electroosmotic flow generated by a porous microneedle array patch, Nat. Commun. 12 (1) (2021) 658.
[13] Y. Kim, H. Lim, E. Lee, Y. Seo, Pigmentation effect of rice bran extract in hair follicle-like tissue and organ culture models, Tissue Eng. Regen. Med. 17 (1) (2020) 15–23.
[14] H. Huang, T. Belwal, L. Li, Y. Xu, L. Zou, X. Lin, Z. Luo, Amphiphilic and biocompatible DNA origami-based emulsion formation and nanopore release for anti-melanogenesis therapy, Small 17 (45) (2021), e2104831.
[15] P. Carter, B. Narasimhan, Q. Wang, Biocompatible nanoparticles and vesicular systems in transdermal drug delivery for various skin diseases, Int. J. Pharm. 555 (2019) 49–62.
[16] A.C. Lee, H. Moon, K. Ishihara, Stabilization of lipid lamellar bilayer structure of stratum corneum modulated by poly(2-methacryloyloxyethyl phosphorylcholine) in relation to skin hydration and skin protection, Tissue Eng. Regen. Med. 18 (6) (2021) 953–962.
[17] A.G. Guex, N. Di Marzio, D. Eglin, M. Alini, T. Serra, The waves that make the pattern: a review on acoustic manipulation in biomedical research, Mater, Today Bio 10 (2021), 100110.
[18] T. Garg, Current nanotechnological approaches for an effective delivery of bio-active drug molecules in the treatment of acne, Artif. Cell Nanomed. Biotechnol. 44 (1) (2016) 98–105.
[19] C. Puglia, F. Bonina, Lipid nanoparticles as novel delivery systems for cosmetics and dermal pharmaceuticals, Expet Opin. Drug Deliv. 9 (4) (2012) 429–441.
[20] W.T. Shen, Y. Wu, H.Q. He, Y. Yu, H.H. Qin, J.B. Fei, G.J. Wang, Efficacy and safety of artemether emulsion for the treatment of mild-to-moderate acne vulgaris: a randomized pilot study, J. Dermatol. Treat. 32 (7) (2021) 762–765.
[21] E. Araviiskaia, J.L. Lopez Estebaranz, C. Pincelli, Dermocosmetics: beneficial adjuncts in the treatment of acne vulgaris, J. Dermatol. Treat. 32 (1) (2021) 3–10.
[22] C.H. Lin, Y.P. Fang, S.A. Al-Suwayeh, S.Y. Yang, J.Y. Fang, Percutaneous absorption and antibacterial activities of lipid nanocarriers loaded with dual drugs for acne treatment, Biol. Pharm. Bull. 36 (2) (2013) 276–286.
[23] Q.Y. Li, J.H. Lee, H.W. Kim, G.Z. Jin, Research models of the nanoparticle-mediated drug delivery across the blood-brain barrier, Tissue Eng. Regen. Med. 18 (6) (2021) 917–930.
[24] L.E. Millikan, Adapalene: an update on newer comparative studies between the various retinoids, Int. J. Dermatol. 39 (10) (2000) 784–788.
[25] H.Y. Lee, S.H. Park, J.H. Kim, M.S. Kim, Temperature-responsive hydrogels via the electrostatic interaction of amphiphilic diblock copolymers with pendant-ion groups, Polym. Chem. 8 (2017) 6606–6616.
[26] H.Y. Lee, J.H. Park, Y.B. Ji, D.Y. Kwon, B.K. Lee, J.H. Kim, K. Park, M.S. Kim, Preparation of pendant group-functionalized amphiphilic diblock copolymers in the presence of a monomer activator and evaluation as temperature-responsive hydrogels, Polymer 137 (2018) 293–302.
[27] M.S. Kim, H. Hyun, K.S. Seo, Y.H. Cho, G. Khang, H.B. Lee, Preparation and characterization of MPEG-PCL diblock copolymers with thermo-responsive sol-gel-sol behavior, J. Polym. Sci. Polym. Chem. 44 (2006) 5413–5423.
[28] J.H. Park, S.H. Park, H.Y. Lee, J.W. Lee, B.K. Lee, B.Y. Lee, J.H. Kim, M.S. Kim, An injectable, electrostatically interacting drug depot for the treatment of rheumatoid arthritis, Biomaterials 154 (2018) 86–98.

[29] J.Y. Seo, B. Lee, T.W. Kang, J.H. Noh, M.J. Kim, Y.B. Ji, H.J. Ju, B.H. Min, M.S. Kim, Electrostatically interactive injectable hydrogels for drug delivery, Tissue Eng. Regen. Med. 15 (5) (2018) 513–520.
[30] N. Contessi Negrini, A. Angelova Volponi, C.A. Higgins, P.T. Sharpe, A.D. Celiz, Scaffold-based developmental tissue engineering strategies for ectodermal organ regeneration, Mater, Today Bio 10 (2021), 100107.
[31] A. Malkawi, A. Jalil, I. Nazir, B. Matuszczak, R. Kennedy, A. Bernkop-Schnurch, Self-emulsifying drug delivery systems: hydrophobic drug polymer complexes provide a sustained release in vitro, Mol. Pharm. 17 (2020) 3709–3719.
[32] H. Lin, Q. Xie, X. Huang, J. Ban, B. Wang, X. Wei, Y. Chen, Z. Lu, Increased skin permeation efficiency of imperatorin via charged ultradeformable lipid vesicles for transdermal delivery, Int. J. Nanomed. 13 (2018) 831–842.
[33] T. Higuchi, Rate of release of medicaments from ointment bases containing drugs in suspensions, J. Pharmacol. Sci. 50 (1961) 874–875.
[34] P. L Ritger, N.A. Peppas, A simple equation for description of solute release. I. Fickian and non-Fickian release from non-swellable devices in the form of slabs, spheres, cylinders or discs, J. Contr. Release 5 (1987) 23–26.